

DNA binding, nuclease activity and cytotoxicity studies of Cu(II) complexes of tridentate ligands

Pankaj Kumar^a, Sukhamoy Gorai^a, Manas Santra^b, Biplab Mondal^{a,*}, Debasis Manna^{a,*}

^aDepartment of Chemistry, Indian Institute of Technology Guwahati, Assam 781039, India

^bNational Center for Cell Science, Pune 411007, Maharashtra, India

Table of Contents	Page
Figure S1. FT-IR spectrum of the L₁ in KBr pellet.	2
Figure S2. Mass spectrum for L₁ in methanol.	2
Figure S3. ¹ H-NMR spectrum of L₁ in CDCl ₃ .	3
Figure S4. ¹³ C-NMR spectrum of L₁ in CDCl ₃ .	3
Figure S5. FT-IR spectrum of the L₂ in KBr pellet.	4
Figure S6. UV-visible spectrum of complex 1 in methanol.	4
Figure S7. X-Band EPR spectrum of complex 1 in methanol at 298K.	5
Figure S8. (A) Representative fluorescence emission spectra of BSA (2 μM) 5 mM Tris-HCl/NaCl buffer (pH 7.2) in presence of complex 1 at room temperature, with the increase in molar ratio of complexes to BSA (0-60). (B) The plot of I ₀ /I vs. [complex] for the Cu(II) complexes.	5
Figure S9: (a) Representative gel electrophoresis diagram showing the time dependent chemical nuclease activity of the complexes (150 μM) using SC pUC19 DNA (30 μM, 0.2 μg) in absence of external agents in 5 mM Tris-HCl/NaCl buffer (pH 7.2) at 37 °C: lane 1-8, DNA + complex (0, 0.5, 1.5, 2.5, 4, 5.5, 7, 9 h). The gel images from A-D are for complex 1-3 respectively.	6
Figure S10: Representative plot of cell viability of complex 2 in a dose dependent manner in human breast (MCF7), lung (A549) and colon (HCT116) cancer cell lines.	7
Table S1: Observed rate constants for the cleavage of supercoiled pUC19 DNA by Cu(II) complexes.	7
Table S2. Chemical nuclease activity of supercoiled pUC19 DNA by the complexes in presence of various additives.	8

Ligand Characterization:

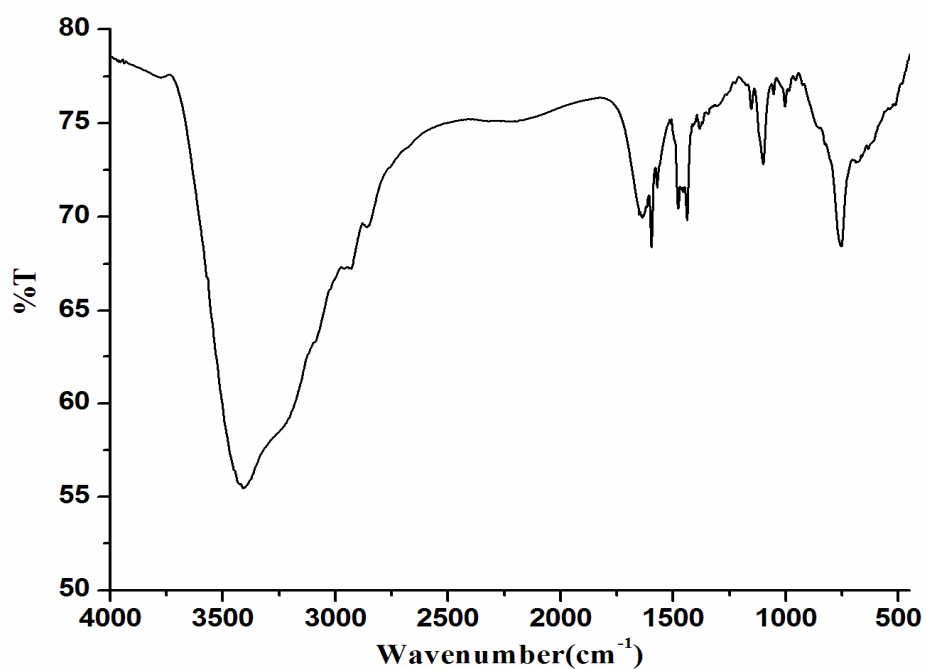


Figure S1. FT-IR spectrum of the \mathbf{L}_1 in KBr pellet.

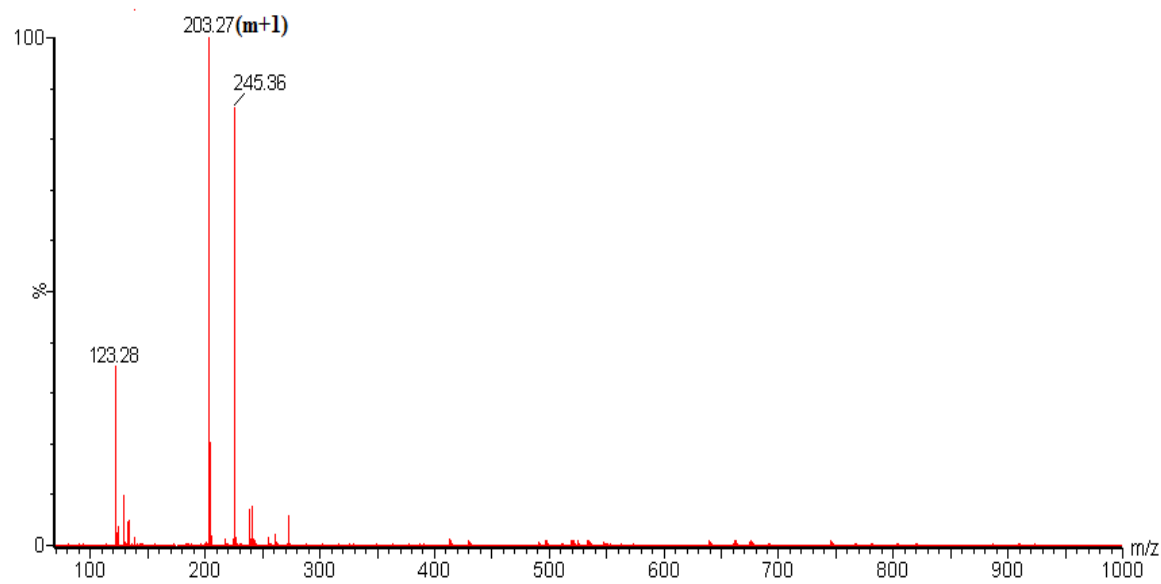


Figure S2. Mass spectrum for \mathbf{L}_1 in methanol.

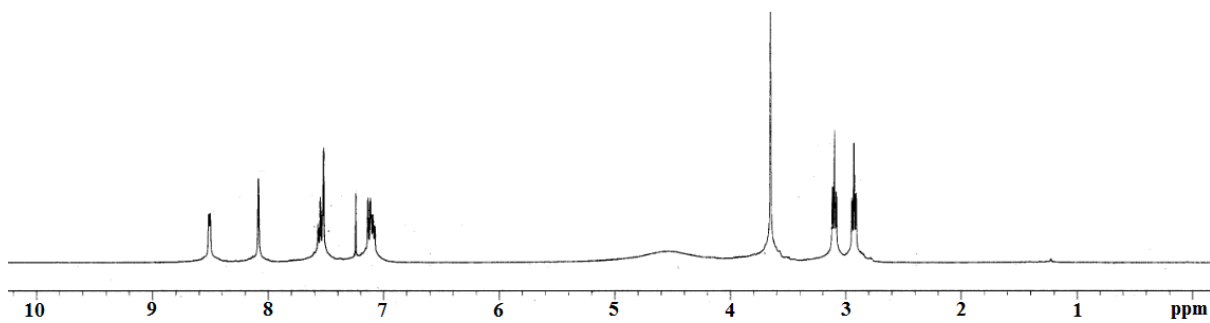


Figure S3. ¹H-NMR spectrum of L₁ in ¹³CDCl₃.

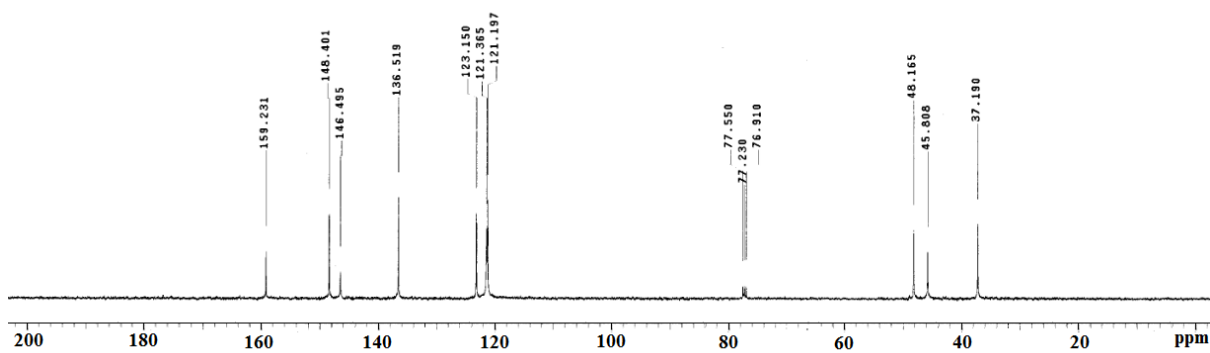


Figure S4. ¹³C-NMR spectrum of L₁ in ¹³CDCl₃.

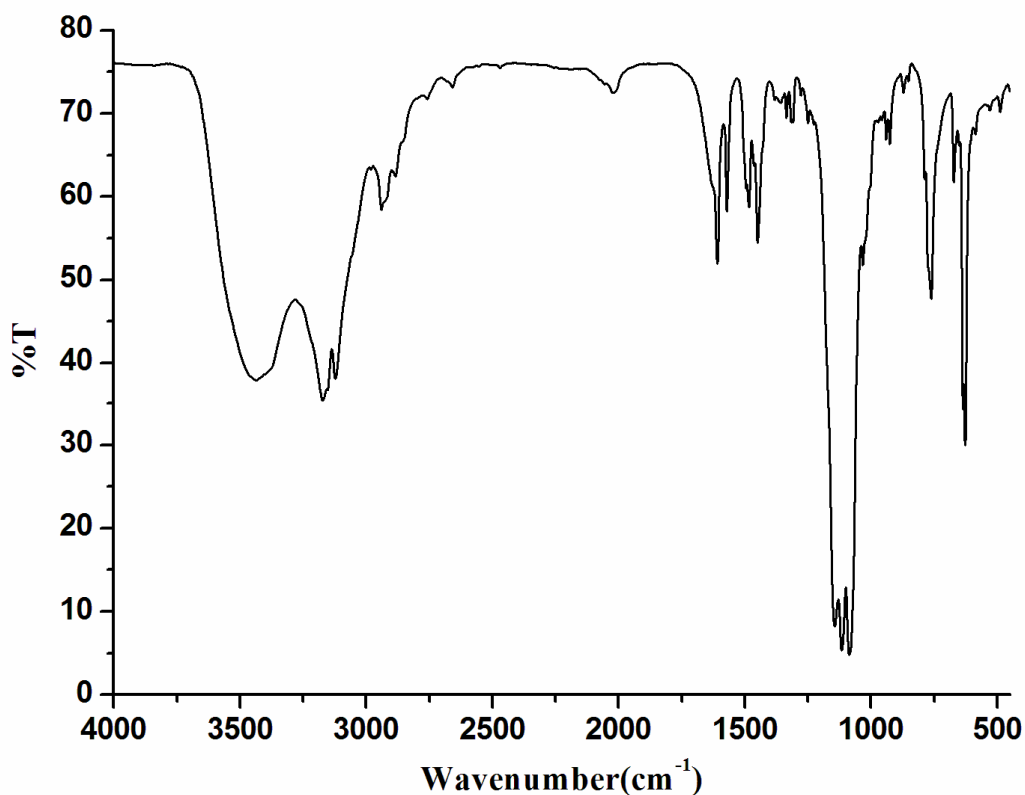


Figure S5. FT-IR spectrum of the complex **1** in KBr pellet.

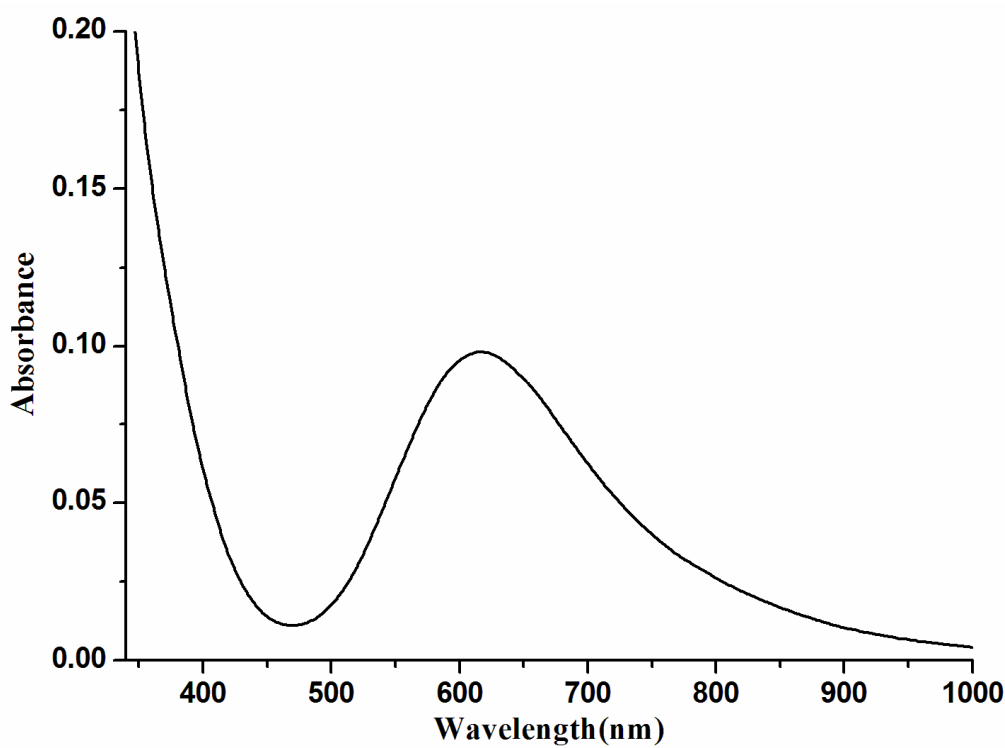


Figure S6. UV-visible spectrum of complex **1** in methanol.

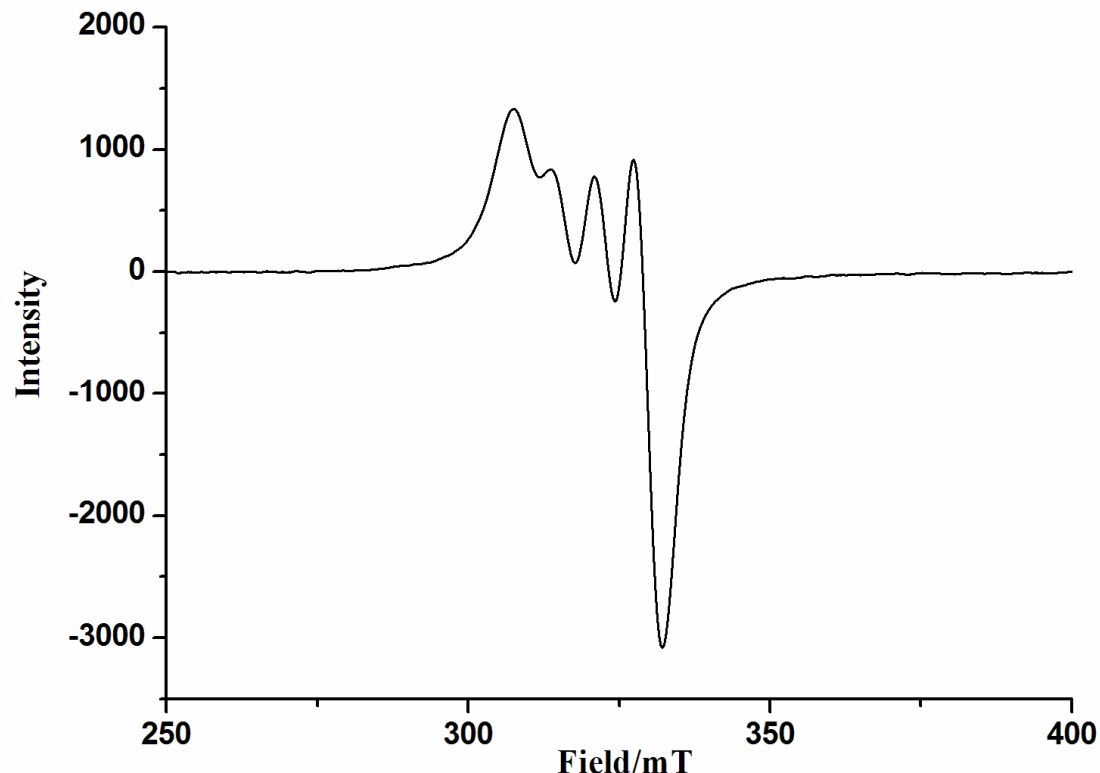


Figure S7. X-Band EPR spectrum of complex **1** in methanol at 298K.

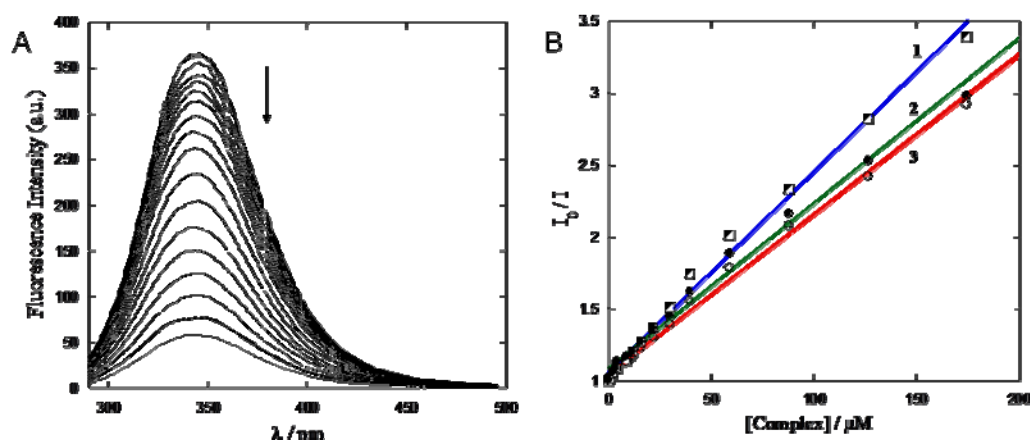


Figure S8: (A) Representative fluorescence emission spectra of BSA (2 μM) 5 mM Tris-HCl/NaCl buffer (pH 7.2) in presence of complex **1** at room temperature, with the increase in molar ratio of complexes to BSA (0-60). (B) The plot of I_0/I vs. [complex] for the Cu(II) complexes.

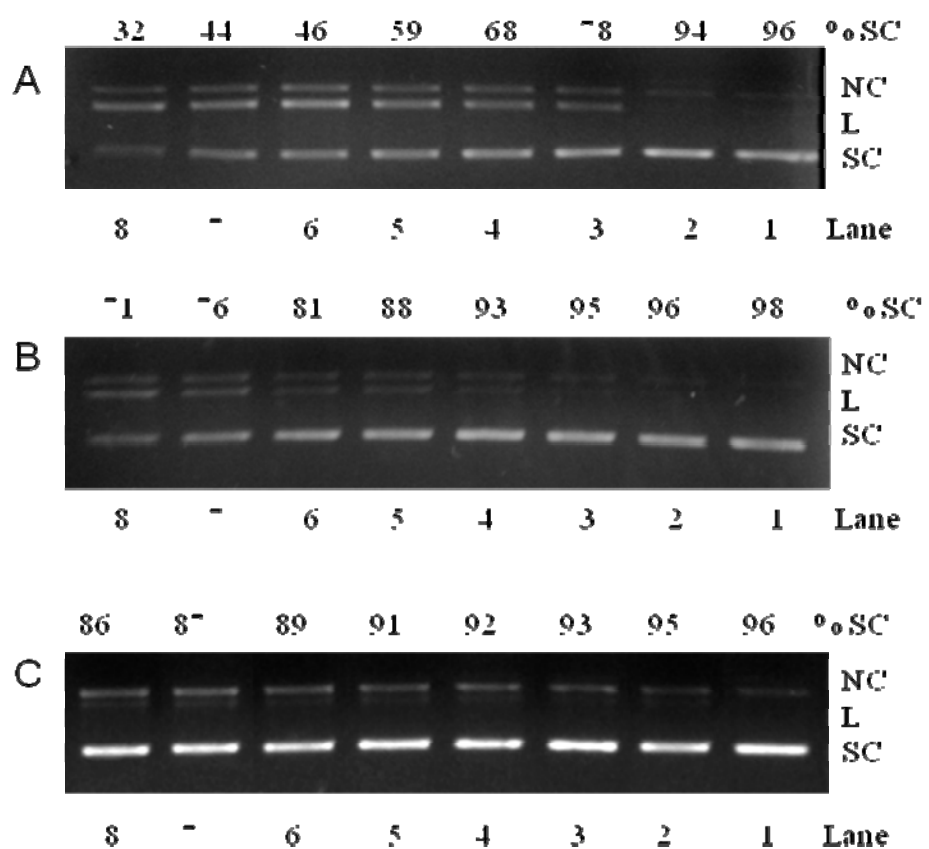


Figure S9: (a) Representative gel electrophoresis diagram showing the time dependent chemical nuclease activity of the complexes (150 μ M) using SC pUC19 DNA (30 μ M, 0.2 μ g) in absence of external agents in 5 mM Tris-HCl/NaCl buffer (pH 7.2) at 37 $^{\circ}$ C: lane 1-8, DNA + complex (0, 0.5, 1.5, 2.5, 4, 5.5, 7, 9 h). The gel images from A-D are for complex **1-3** respectively.

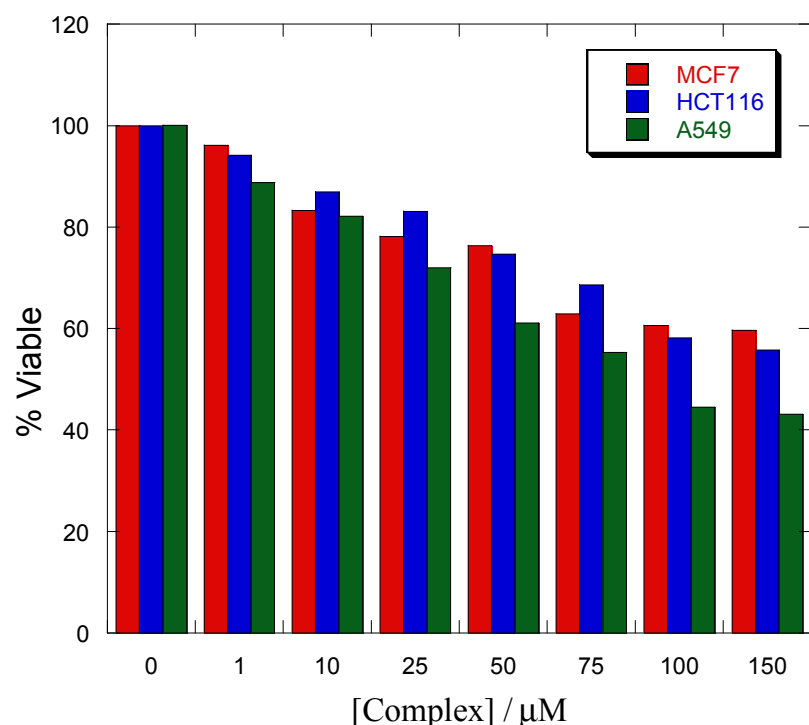


Figure S10: Representative plot of cell viability of complex **2** in a dose dependent manner in human breast (MCF7), lung (A549) and colon (HCT116) cancer cell lines.

Table S1: Observed rate constants for the cleavage of supercoiled pUC19 DNA by Cu(II) complexes.

^a Complex	1	2	3
K_{obs}/s^{-1}	$3.37 (\pm 0.15) \times 10^{-5}$	$1.02 (\pm 0.053) \times 10^{-5}$	$3.21 (\pm 0.15) \times 10^{-6}$

^a[complex] = 150 μM . [DNA] = 30 μM

Table S2. Chemical nuclease activity of supercoiled pUC19 DNA by the complexes in presence of various additives.

Complex	% SC DNA							
	DNA Only	complex + MPA	complex + H ₂ O ₂	complex + DMSO ^a	+NaN ₃ ^b	+KI ^c	+L-histidine ^d	
1	82	67	6	25	96	61	19	8
2	86	83	2	64	92	57	32	40
3	96	86	3	46	59	4	21	6

[complex] = 50 μM. ^aDMSO = 6 μL. ^b[NaN₃] = 500 μM. ^c[KI] = 500 μM. ^d[L-histidine] = 500 μM.